AAC Accepts, published online ahead of print on 8 December 2014
Antimicrob. Agents Chemother. doi:10.1128/AAC.03659-14




# The Antiviral Potential of ERK/MAPK and PI3K/AKT/mTOR Signaling Modulation for MERS-CoV Infection as Identified by Temporal Kinome Analysis

**Running Title:** Kinome analysis of MERS-CoV infection

Jason Kindrachuk[1¶], Britini Ork[1], Brit J. Hart[1], Steve Mazur[1], Michael R. Holbrook[1], Matthew B. Frieman[2], Dawn Traynor[1], Reed F. Johnson[3], Julie Dyall[1], Jens H. Kuhn[1], Gene G. Olinger[1], Lisa E. Hensley[1], and Peter B. Jahrling[1,3]

[1] Integrated Research Facility, National Institute of Allergy and Infectious Diseases, National Institutes of Health, Frederick, Maryland, United States of America

[2]Department of Microbiology and Immunology, University of Maryland at Baltimore, Baltimore, Maryland, United States of America

[3]Emerging Viral Pathogens Section, National Institute of Allergy and Infectious Diseases, National Institutes of Health, Frederick, Maryland, United States of America

¶ Corresponding author: Mailing address: Integrated Research Facility at Fort Detrick, National Institutes of Health (NIH), National Institute of Allergy and Infectious Diseases (NIAID), 8200 Research Plaza, Frederick, MD, USA, 21702. E-mail: kindrachuk.kenneth@nih.gov

**Disclaimer:** The content of this publication does not necessarily reflect the views or policies of the US Department of Health and Human Services or of the institutions and companies affiliated with the authors.

**Abstract**

Middle East respiratory syndrome coronavirus (MERS-CoV) is a lineage-C betacoronavirus and infections with this virus can result in acute respiratory syndrome with renal failure. Globally, MERS-CoV has been responsible for 877 laboratory-confirmed infections, including 317 deaths, since Septermber, 2012. As there is a paucity of information regarding the molecular pathogenesis associated with this virus, or the identities of novel antiviral drug targets we performed temporal kinome analysis on human hepatocytes infected with the Erasmus isolate of MERS-CoV (MERS-CoV) with peptide kinome arrays. Bioinformatic analysis of our kinome data, including pathway over-representation analysis (ORA) and functional network analysis, suggested that ERK/MAPK and PI3K/AKT/mTOR signaling responses were specifically modulated in response to MERS-CoV infection *in vitro* throughout the course of infection. The over-representation of specific intermediates within these pathways following pathway and functional network analysis of our kinome data correlated with similar patterns of phosphorylation through western blot array analysis. In addition, analysis of the effects of specific kinase inhibitors on MERS-CoV infection in tissue culture models confirmed these cellular response observations. Further, we have demonstrated that a subset of licensed kinase inhibitors targeting the ERK/MAPK and PI3K/AKT/mTOR pathways significantly inhibited MERS-CoV replication *in vitro* whether added pre- or post-viral infection. Taken together, our data suggests that ERK/MAPK and PI3K/AKT/mTOR signaling responses play important roles in MERS-CoV infection and may represent novel drug targets for therapeutic intervention strategies.

## Introduction

Middle East respiratory syndrome is a viral respiratory disease that results from infection with the MERS coronavirus (MERS-CoV), was first identified in a patient with acute pneumonia and renal failure in Jeddah, Kingdom of Saudi Arabia in June 2012 (1). Subsequently, there have been 877 laboratory-confirmed MERS-CoV infections to date, including 317 deaths (http://www.who.int/csr/don/16-october-2014-mers/en/), resulting in a case fatality rate of 30%, with all cases directly or indirectly linked to the Middle East region (2). Recent announcements of laboratory-confirmed MERS-CoV infection in patients in the United States and the Netherlands have further exacerbated concerns regarding the global evolution of this epidemic (3).

MERS-CoV belongs to the same genus (betacoronavirus) as severe acute respiratory syndrome coronavirus (SARS-CoV), which was responsible for the global SARS pandemic of 2002-2003 that affected more than 8,000 people (4), and the human CoVs HKU1 and OC43, which cause mild to moderate respiratory disease (5). Further, MERS-CoV is the first lineage 2c betacoronavirus shown to infect humans (6, 7). Although the natural reservoir for MERS-CoV has yet to be determined, it has been suggested that bats are a likely candidate given the similarity of MERS-CoV to bat coronaviruses (8). Recent evidence has also suggested that dromedary camels may act as an intermediate host for MERS-CoV as supported by serological, genetic and epidemiological evidence as well as the recent isolation of virus (9, 10). Animal-to-human transmission has been largely suspected as the primary contributor to the recent outbreaks of MERS-CoV. Although human-to-human transmission has been reported in several case clusters there is currently no evidence for sustained community transmission (11). MERS-CoV

infections have been associated with severe lower respiratory tract infections, including acute respiratory syndrome with renal failure. Interestingly, the severity of disease presentation appears to be related to underlying comorbidities as MERS-CoV infections in healthy individuals appear to result primarily in mild to asymptomatic disease (1, 12, 13).

Though appreciable efforts have been made to identify novel antiviral therapeutics for MERS-CoV there are currently no approved therapeutic interventions available and treatment is based on supportive care (14). Initial investigations of interferon demonstrated that IFN-α, IFN-γ and IFN-ß were able to inhibit MERS-CoV replication (15, 16). Subsequent studies demonstrated that amongst different interferons, IFN-ß had the strongest inhibitory activity against MERS-CoV (17). Mycophenolic acid, IFN-β and ribavirin have demonstrated strong inhibitory activities against MERS-COV *in vitro* (17, 18) and Falzarano et al. demonstrated that the administration of IFN-α2b and ribavirin resulted in synergistic antiviral activities both *in vitro* and *in vivo* in rhesus macaques (19). Josset and colleagues employed systems-level gene expression analysis of MERS-CoV infection *in vitro* and identified that IFN-α5 and IFN-β were specifically up-regulated by MERS-CoV infection (20).

Surveys of the host response to infection through either genomic or proteomic technologies have been previously employed to characterize microbial pathogenesis and identify novel therapeutic targets (21-24). The incorporation of systems-level analysis to such investigations provides a unique opportunity to identify specific host or pathogen responses that are modulated during the course of infection. A global transcriptome analysis of host responses to MERS-CoV and SARS-CoV infection suggested that MERS-CoV differently modulated transcriptional changes in the host although viral replication kinetics were similar for both viruses (20). Subsequent systems-level analysis of the transcriptome datasuggested that changes

116 in the host transcriptome to either MERS-CoV or SARS-CoV may be related to the activation
117 state of cell signaling networks. Further, the authors demonstrated that the identification of
118 specific cellular intermediates through upstream regulator analysisUpstream could be used to
119 predict potential host targets for therapeutic intervention. However, many cellular processes are
120 regulated independent of changes in transcriptional or translational regulation through kinase-
121 mediated modulation of cell signaling networks. Characterization of the activation state of
122 cellular host kinases, or the kinome, provides a mechanism to identify the individual kinases
123 and/or signaling networks that are of central importance to disease progression or resolution.
124 Previously, we demonstrated the utility of species-specific kinome analysis with peptide kinome
125 arrays for characterizing the modulation of host cell signaling networks, including infectious
126 disease (25, 26).

127 Here, we have characterized the temporal host kinome response of human hepatocytes to
128 the infection with MERS-CoV isolate HCoV-EMC/2012 (MERS-CoV) and identified specific
129 cell signaling networks and kinases that are modulated during the course of infection and may
130 represent novel antiviral targets. As it has been previously demonstrated that HUH7 hepatocytes
131 are highly permissive to MERS-CoV (27), and it is postulated that targets found to be over-
132 represented in our data sets would potentially represent conserved targets across multiple
133 permissive cell types, we have focused on these cells for our analysis. Subsequent systems
134 biology approaches, including pathway over-representation analysis (ORA) and functional
135 network analysis, were used to identify and compare the specific kinome and cell signaling
136 responses that were modulated throughout the course of MERS-CoV infection. Analysis of our
137 kinome data suggested that ERK/MAPK and PI3K/AKT/mTOR signaling responses were
138 specifically modulated in response to MERS-CoV infection *in vitro*. The phosphorylation of

specific intermediates within these pathways in the kinome array data correlated with similar phosphorylation patterns from western blot dot arrays. In addition, we confirmed these cellular responses through analysis of the effects of inhibition of these pathways, or their intermediates, on MERS-CoV infection in tissue culture models. Further, we have demonstrated that a subset of the licensed kinase inhibitors targeting the ERK/MAPK and PI3K/AKT/mTOR pathways significantly inhibited MERS-CoV propagation *in vitro* whether added pre- or post-viral infection. Taken together, our investigation has demonstrated that ERK/MAPK and PI3K/AKT/mTOR signaling responses play a critical role in MERS-CoV pathogenesis and may be potential targets for therapeutic intervention strategies.

## Materials and Methods

### Cells and Virus

HUH7 cells are a hepatocyte derived epithelial-like cell line and were maintained in Dulbecco's minimal essential medium (DMEM) (Sigma-Aldrich) supplemented with 10% (v/v) heat inactivated fetal bovine serum (FBS) in a 37 °C humidified 5% (v/v) $CO_2$ incubator. MERS-CoV isolate HCoV-EMC/2012 (MERS-CoV), kindly provided by Rocky Mountain Laboratories (NIH/NIAID) and the Viroscience Laboratory, Erasmus Medical Center (Rotterdam, Netherlands), was used for all experiments and propogated as reported previously (28).

### Chemical Inhibitors

The FDA licensed drugs tested (sorafenib, everlimus, dabrafenib, cabozantinib, afatanib, selumetinib, trametinib, and miltefosine) were purchased from Selleck Chemicals. Additional kinase inhibitors tested included, AG490, PKC-412, GF109203X, SB203580, wortmannin, Bay

11-7082, GW5074, PP2, and rapamycin (sirolimus) as well as an inhibitor of nitric oxide synthase 2 (NOS2), L-NAME. All were purchased from Enzo Scientific. Inhibitiors were reconstituted according to manufacture recommendations in either water or DMSO.

**Viral Infections for Kinome Analysis**

HUH7 cells were plated in 6-well plates in fresh DMEM supplemented with 2% (v/v) FBS and rested for 24 hours prior to infection. Cells were infected with MERS-CoV at a multiplicity of infection (MOI) of 0.05 for 1 hour at 37 °C, 5% $CO_2$ with periodic rocking. Following incubation, HUH7 cells were washed twice with phosphate-buffered saline (PBS) to remove unbound virus and replenished with fresh DMEM supplemented with 2% (v/v) FBS and incubated at 37 °C/5% $CO_2$. MERS-CoV- infected and mock-infected cells and cell culture supernatant were harvested at identified time points (1, 6, 24 hr p.i.) for subsequent kinome analysis. Plaque assays were performed on VERO E6 as reported previously (17).

**Kinome Analysis with Peptide Arrays**

Design, construction and application of peptide arrays were based upon a previously reported protocol (29). Briefly, MERS-CoV-infected and mock-infected HUH7 cells were scraped and pelleted at 1, 6 and 24 hr p.i. Following this, cell supernatants were discarded and the cell pellets were lysed with 100 µL of lysis buffer (20 mM Tris-HCl, pH 7.5, 150 mM NaCl, 1 mM ethylenediamine tetraacetic acid (EDTA), 1 mM ethylene glycol tetraacetic acid (EGTA), 1% Triton-X100, 2.5 mM sodium pyrophosphate, 1 mM $Na_3VO_4$, 1 mM NaF, 1 µg/mL leupeptin, 1 µg/mL aprotinin, 1 mM phenylmethylsulfonyl fluoride) and incubated on ice for 10 min followed by centrifugation to remove cell debris. Cell lysates were transferred to fresh

microcentrifuge tubes and the total protein from the cell lysates was measured using a BCA assay (Pierce) to calculate cell lysate volumes to ensure equal total protein loading onto arrays. Activation mix (50% glycerol, 50 µM ATP, 60 mM $MgCl_2$, 0.05% Brij-35 and 0.25 mg/mL bovine serum albumin) was added to the cell lysate fractions and were spotted onto human kinome arrays (JPT Technologies) and incubated for 2 hr at 37 °C as described previously (22). Kinome arrays were subsequently washed once with PBS containing 1% Triton X-100 followed by a single wash in deionized $H_20$. Peptide arrays were held on dry ice and subjected to gamma-irradiation (5 MRad) to inactivate any residual virus following removal from biocontainment. Kinome arrays were submerged in PRO-Q Diamond Phosphoprotein Stain (Invitrogen) with gentle agitation in the dark for 1 hr. Following staining, arrays were washed in destain [20% acetonitrile, 50 mM sodium acetate, pH 4.0 (Sigma-Aldrich)] 3 times for 10 minutes per wash with the addition of fresh destain each time. A final wash was performed with $dH_2O$ and placed in 50 mL conical tubes to air dry for 20 minutes. Remaining moisture was removed by centrifugation of the arrays at 300 x g for 3 min. Array images were acquired using a PowerScanner microarray scanner (Tecan) at 532-560 nm with a 580 nm filter to detect dye fluorescence. Images were collected using the GenePix 6.0 software (MDS). Signal intensity values were collected using the GenePix 6.0 Software (MDS). All data processing and subsequent analysis was performed using the Platform for Integrated, Intelligent Kinome Analysis (PIIKA) software (http://saphire.usask.ca/saphire/piika) (29, 30) as described previously (22).

**Pathway Over-Representation Analysis and Functional Network Analysis**

Pathway over-representation analysis of differentially phosphorylated proteins was performed usingInnateDb (http://www.innatedb.com), a publically available resource that predicts biological pathways based on experimental fold change datasets in humans, mice and bovines (31). Pathways are assigned a probability value (p) based on the number of genes present for a particular pathway as well as the degree to which they are differentially expressed or modified relative to a control condition. For our investigation, input data was limited to peptides that demonstrated consistent responses across the biological replicates ($p<0.05$) as well as statistically significant changes from the control condition ($p<0.20$) as reported previously (29). Additionally, functional networks were created using Ingenuity Pathway Analysis (IPA) software (Ingenuity Systems, Redwood City, CA). Proteins IDs and the respective phosphorylation fold-change values and p-values were uploaded and mapped to their corresponding protein objects in the IPA Knowledge Base. Networks of these proteins were algorithmically generated based on their connectivity and assigned a score. Proteins are represented as nodes, and the biological relationship between two nodes is represented as an edge (solid line for direct relationships and a dotted line for indirect relationships). The intensity of the node color indicates the degree of up (red)- or down (green)-regulation of phosphorylation. Proteins in uncolored nodes were not identified as differentially expressed in our experiment and were integrated into the computationally generated networks on the basis of the evidence stored in the IPA knowledge database indicating a relevance to this network.

**Western Blot Array Analysis of Protein Phosphorylation**

HUH7 cells were infected with MERS-CoV or mock-infected as described above. Cells from infected or mock-infected cells were harvested at 1, 6 or 24 hr p.i. and lysed in SDS loading

buffer without bromophenol blue (200 mM Tris-HCl, pH 6.8; 8% SDS; 40% glycerol; 4% β-mercaptoethanol; 50 mM EDTA) and boiled for 20 min at 95 °C to inactivate remaining virus (as approved within our Standard Operating Procedures). Following inactivation, supernatants were removed from biocontainment and boiled again for 20 min at 95 °C for subsequent analysis. Protein concentration was determined using the BCA Protein Assay kit (Pierce), according to the manufacturer's instructions. Equal amounts of protein from mock-infected or MERS-CoV-infected samples were loaded onto PathScan Intracellular Signaling Antibody Array membranes (Cell Signaling Technologies) and analyzed according to the manufacturer's instructions. Images were acquired using a Syngene G:Box Chemi (Syngene) and quantification of antibody spot intensities was determined using the ImageJ software suite (32).

**Cytotoxicity Assays**

Kinase inhibitor cytotoxicity was determined using the Cytotox colormetric assay measuring lactate dehydrogenase (LDH) (Promega) released from treated cells following the manufacturer's instructions. HUH7 cells were incubated with each of the drugs for 24 hr in a 37 °C, 5% $CO_2$ incubator using inhibition assay inhibitor concentrations. The cell culture supernatents were then used in the Cytotox 96 well assay and adsorbance was read at 490nm with a M1000 Tecan plate reader.

**Cell-Based ELISA for Analysis of Inhibition of MERS-CoV Infection by Kinase Inhibitors**

HUH7 cells were plated in black, opaque bottom 96-well plates and allowed to rest for 24 hr prior to infection and treatments. The cells were either pre-treated 1 hr prior to infection or 2 hr post-infection with kinase inhibitors at final concentrations of 0.1, 1, and 10 μM. The final

concentration of DMSO was 0.1% for all experimental conditions. Cells were infected with MERS-CoV at a MOI of 0.05 and allowed to incubate for 48 hr at 37 °C, 5% $CO_2$ prior to fixation. After 48 hr, the cells were fixed with 10% neutral buffered formalin (NBF) for 30 min, the NBF was changed and the cells fixed for an additional 24 hr at 4 °C to ensure viral inactivation following facility-specific Standard Operating Procedures. Viral inhibition was then determined utilizing a cell-based enzyme linked immosorbent assay (ELISA) as described by Hart et al (17).

**Plaque Reduction Assay for Analysis of Inhibition of MERS-CoV Infection by Kinase Inhibitors**

To determine the antiviral activity of kinase inhibitors, HUH7 cells were incubated with select kinase inhibitors (10 μM) for 1 hr prior to infection with MERS-CoV. Cells were infected with MERS-CoV at a multiplicity of infection (MOI) of 0.05 for 1 hr at 37 °C, 5% $CO_2$ with periodic rocking. Following incubation, HUH7 cells were washed twice with phosphate-buffered saline (PBS) to remove unbound virus and replenished with fresh DMEM supplemented with 2% (v/v) FBS and incubated at 37 °C/5% $CO_2$ with or without readministration of the same kinase inhibitors (10 μM). Cell supernatants from the infected and mock-infected cells were harvested 48 hr p.i. and the inhibitory activity of the kinase inhibitor-treated cells was assessed by plaque reduction assay as described previously (17).

**Results**

**Temporal Kinome Analysis of MERS-CoV-Infected Hepatocytes**

To gain insight into potential host signaling networks or kinases that are modulated during MERS-CoV infection, and that may represent novel therapeutic targets, we performed temporal kinome analysis of MERS-CoV-infected HUH7 human hepatocytes. Previously, de Wilde et al. demonstrated that HUH7 cells were highly permissive to MERS-CoV infection (27) and we postulated that host signaling networks or individual proteins identified by our analysis may be broadly conserved across multiple cell types targeted by MERS-CoV. In addition, we employed a low multiplicity of infection (MOI=0.01) to identify host signaling networks or intermediates in an effort to recapitulate circumstances in which host cells would encounter low amounts of virus (ie. During the initial phases of natural infection). Cells were harvested at multiple time points (1, 6 and 24 hr) postinfection (p.i.) alongside time-matched, mock-infected control cells. Kinome analysis with peptide arrays relies on the phosphorylation of specific kinase targets (immobilized peptides) on the arrays by active kinases in a cell lysate (22). Our arrays contained 340 unique peptides representing key phosphorylation events from a broad spectrum of cell signaling pathways and processes. The kinome data was extracted from the arrays and analyzed using the PIIKA software tool (29, 30). Hierarchical clustering analysis demonstrated that the MERS-CoV-infected 1 hr p.i. sample clustered between the mock samples whereas the 6 hr and 24 hr p.i. MERS-CoV samples clustered outside of the mock-infected samples suggesting an increased diversity in the host response from the mock at these time points (Figure 1A). Clustering analysis of the kinome data following biological subtraction of the time-matched mock-infected kinome data sets from their MERS-CoV counterparts is presented in Figure 1B. Further, principal component analysis (PCA) of the mock- and MERS-CoV -infected kinome data demonstrated complete separation of the data sets into two individual clusters (Figure 1C). Titration of cell culture supernatants from our kinome analysis by plaque assay also

298 demonstrated that these cells were productively infected during the course of our analysis
299 (Figure 1D). It should be noted that the viral titers determined at 1 hr p.i. represent the amount
300 of virus remaining in the supernatant at this time point prior to washing of the cells.
301
302 **Systems Analysis of Temporal Kinome Data**
303 To gain biological insight into the molecular host response to MERS-CoV infection we
304 employed pathway over-representation analysis (ORA) with both the InnateDB and IPA
305 software suites. Pathway over-representation analysis with InnateDB was performed in an effort
306 to identify specific signaling pathways that were modulated throughout the course of MERS-
307 CoV infection. Analysis of the upregulated signaling pathways at all time-points demonstrated
308 that MERS -CoV infection modulated a broad range of cellular functions (Supplemental Table
309 1). Pathway ORA demonstrated that infection resulted in the modulation of host signaling
310 pathways 1 hr p.i. Notably, multiple cell signaling pathways related to cell proliferation
311 (cancer/carcinoma, growth factor signaling) and cell growth and differentiation (p53 effectors,
312 Wnt signaling) were upregulated while multiple pro-inflammatory [tumor necrosis factor (TNF),
313 and interleukin (IL)-1] and innate immune response signaling pathways (Toll-like receptor
314 signaling) were downregulated at this time point. The signaling pathways modulated at 6 hr and
315 24 hr p.i. decreased in overall breadth and complexity as compared to the number of pathways
316 identified at the 1 hr time point (Supplemental Table 1). In particular, by the 24 hr time point the
317 majority of upregulated signaling pathways were related to cell junctions (adherens junction and
318 tight junction pathways), Wnt-,TGFβ- or PI3K/AKT/mTOR-mediated signaling responses with
319 concomitant downregulation of multiple innate immune response-related signaling pathways
320 including interleukin-, interferon- and TLR-related signaling (Supplemental Table 1). We also

observed specific trends within the signaling pathway data sets for each of the three time points. Pathways at the 1 hr p.i. time point had an over-representation of PI3K/AKT/mTOR (including AKT1, mTOR, PDPK1, PIK3R1, PIK3R2 and RPS6KB1), ERK/MAPK (including MAP2K1, MAPK3 and MAPK14) and NFκB (IKBKB, IKBKG and NFKB1) pathway intermediates within many of the signaling pathways identified. These trends also appeared to be largely conserved in both the 6 hr and 24 hr p.i. signaling pathway data suggesting a potentially critical role for these pathways and intermediates in MERS-CoV infection. These signaling pathway trends were also confirmed by kinome analysis 24 hr p.i. in MRC5 cells providing further evidence for a central role for PI3K/AKT/mTOR and ERK/MAPK signaling intermediates (Data Not Shown). Although these pathway identities were informative, we sought further insight into a broader biological role for these intermediates through functional network analysis (FNA) using the Ingenuity Pathway Analysis software suite. FNA does not limit genes or proteins to specific signaling pathways and instead provides predicted biological networks in which signaling intermediates are grouped based on similarities in overall cellular responses and direct or indirect molecular interactions. The top 2 functional networks for each time point are presented in Figure 2. FNA demonstrated that multiple intermediates within the ERK/MAPK [including ERK1 (MAP2K1), p38 (MAPK14) and MEK] and PI3K/AKT/mTOR signaling pathways were conserved across multiple time points (Figure 2A-C). It was also noted that ERK1/2 formed central nodes at both 1 hr (Figure 2A.ii) and 24 hr (Figure 2C.ii) post-infection while AKT, PI3K and mTOR formed a central core of the top network found 24 hr post-infection (Figure 2C.i).

Comparative analysis of the significantly modulated phosphorylation events from our MERS-CoV kinome data by Venn analysis demonstrated that 14 kinases were conserved amongst data sets from the three p.i. time points (Supplemental Table 2; Supplemental Figure

1A). Interestingly, FNA of this peptide list resulted in multiple ERK/MAPK and PI3K/AKT/mTOR signaling pathway intermediates forming central components of the network further suggesting that these pathways may be important components of the cellular events that accompany MERS-CoV infection (Supplemental Figure 1B). The associated biological functions of this network were identified as cellular movement, cell death and survival and cell cycle.

Based on the trends discovered in our systems analysis of the kinome data, we chose to focus primarily on those signaling pathways or intermediates that were identified as being broadly conserved across our kinome analysis. Western blot analysis with phospho-western blot arrays demonstrated that MERS-CoV infection resulted in the modulation of ERK1/2 phosphorylation in a pattern that matched that found on the kinome arrays. The pattern of mTOR and AKT phosphorylation also matched those found from our kinome analysis. Further, the phosphorylation of, downstream targets of mTOR, including S6 ribosomal protein (S6RP) and p70S6 kinase (P70S6K), were also upregulated in a pattern that largely matched that of mTOR phosphorylation (Figure 3A-C). Importantly, this type of phosphorylation analysis is largely qualitative rather than quantitative; however, the overall trends from our kinome analysis were in agreement with the trends found in our western blot array analysis.

**Kinase Inhibitors Targeting PI3K/AKT/mTOR and ERK/MAPK Signaling Inhibit MERS-CoV Infection**

Following our bioinformaticanalysis of the kinome data we sought further insight into the relationship between the host kinases or signaling networks that were over-represented in our kinome data. As ERK/MAPK and PI3K/AKT/mTOR formed central components of multiple functional networks and signaling pathways within our analysis, we assessed the effect of

selective inhibition of these kinases on MERS-CoV infection through a modified ELISA assay. Using our modified ELISA we previously demonstrated that inhibition of MERS-CoV correlated with decreased viral titers through traditional plaque reduction assays (17). Thus, we chose to assess the effect of select kinase inhibitors targeting the PI3/AKT and ERK/MAPK pathways against MERS-CoV infection through this assay. We also selected inhibitors for specific kinases or signaling pathways identified from individual time points in our analysis (including protein kinase C (PKC)-, NFκB-, nitric oxide synthase (NOS)- and Src-mediated signaling responses). These host components were either found within the functional networks formed from our kinome data or were present within signaling pathways found in our pathway ORA. Importantly, at the highest concentration of kinase inhibitors tested (10 μM) all kinase inhibitors, with the exception of PKC-412 and Ro 31-8220 (20% and 23% cytotoxicity, respectively), had negligible (<10%) cytotoxic effects as assessed by measurement of lactate dehydrogenase which is released during cell lysis (Data not shown). For our analysis we first examined the effects of kinase inhibitors when added 1 hr prior to MERS-CoV infection *in vitro* using the same MOI as that used for the generation of the kinome data (MOI=0.05). Inhibition of PI3K/AKT signaling with wortmannin resulted in 40% inhibition of MERS -CoV infection at the highest concentration tested and decreased to 22% at sub-micromolar concentrations (Figure 4A). In addition, treatment of cells with rapamycin, an inhibitor of mTOR, inhibited MERS-CoV infection by 61% at 10 μM and 24% inhibition at the lowest concentration tested (0.1 μM). Inhibitors for additional kinases that did not form critical components of signaling and/or functional network were also examined and had negligible effects on MERS-CoV infection. Taken together, this data provided further support for a role for the PI3K/AKT/ mTOR signaling pathway during MERS-CoV infection.

Next, we examined the effects of ERK/MAPK pathway inhibitors. Pre-treatment of cells with inhibitors of ERK/MAPK signaling resulted in the inhibition of MERS-CoV infection: SB203580 (p38 MAPK) and U0126 (MEK1/2) with similar inhibitory activities against MERS-CoV at 10 μM (45% and 51% inhibition, respectively). Pre-treatment of cells with 10 μM of GW5074, an inhibitor of Raf, a kinase that is involved in the ERK/MAPK signaling transduction cascade and was present in multiple signaling pathways identified from the 6 hr and 24 hr p.i. kinome array data, inhibited MERS-CoV by 52%. This also supported the findings from the analysis of the kinome data in regards to the modulation of ERK/MAPK signaling during MERS-CoV infection.

Inhibition of PKC prior to viral infection also resulted in inhibition of MERS-CoV (Figure 3A). The PKC inhibitors PKC-412, GF109203X and Ro 31-8220 inhibited MERS-CoV infection by 37%, 54% and 74%, respectively, suggesting that PKC also plays an important role during infection. Inhibition of MERS-CoV infection by Ro 31-8220 and GF109203X were significantly greater than that of PKC-412 ($p<0.1$). To examine the role for NFκB signaling in MERS-CoV infection, cells were also pre-treated with Bay 11-7082, an inhibitor of NFκB DNA binding and tumor necrosis factor (TNF)-α induced IκBα phosphorylation, inhibited MERS-CoV infection by 28%. MERS-CoV was largely insensitive (<25% inhibition) to pre-treatment of cells with inhibitors for Src (PP2), EGFR (AG490) or NOS2 (L-NAME) (Figure 4A).

To further assess the role for these kinases or signaling pathways in MERS-CoV infection we selected inhibitors from our pre-treatment experiments with inhibitory activities ≥40% to examine the retention of these activities when added to the cells 2hr p.i. Inhibitors that fit into this classification included inhibitors of PI3K (wortmannin), mTOR (rapamycin), MEK1/2 (U0126), PKC (Ro 31-8220; GF109203X) and c-Raf1 (GW5074). Addition of

413 inhibitors from this subset to the cells 2 hr p.i. largely resulted in decreased inhibitory activity
414 against MERS-CoV infection as compared to pre-infection treatments. Post-infection treatment
415 of cells with rapamycin (mTOR; 57%) had a significantly stronger inhibitory effect on infection
416 as compared to wortmannin (PI3K; 25%) suggesting a more central role for mTOR during
417 MERS-CoV infection as compared to PI3K ($p<0.05$). Post-treatment of infected cells with Ro
418 31-8220 resulted in modest conservation of inhibitory activity (46%), which was similar to that
419 for GF109203X (56%) and rapamycin (Figure 3B).

420 As these analyses provided further support for the role of the ERK/MAPK and
421 PI3K/AKT/mTOR signaling pathways initially identified from our kinome analysis, we
422 postulated that licensed therapeutics targeting these same pathways would also have inhibitory
423 activity against MERS-CoV infections. Here, we selected inhibitors targeting AKT (miltefosine),
424 mTOR (everolimus), ERK/MAPK (selumetinib, trametinib) and Raf (dabrafenib, sorafenib).
425 Cells were treated with inhibitors prior to (1 hr) or following (2 hr) MERS-CoV infection. For
426 kinase inhibitors targeting the ERK/MAPK signal pathway, selumetinib (MEK1; ERK1/2) and
427 trametinib (MEK1/2) had the strongest inhibitory activities of all the inhibitors tested (≥95%),
428 including non-ERK/MAPK inhibitors, whether added prior to (-1 hr; Figure 4A) or following
429 (+2 hr; Figure 5B) infection. Interestingly, trametinib demonstrated significantly stronger
430 inhibitory activity against MERS-CoV than selumetinib at the lowest concentration tested when
431 inhibitors were added prior to infection ($p<0.05$) or at a post-infection treatment concentration of
432 10 μM ($p<0.05$). This suggests that these specific nodes of the ERK/MAPK signaling pathway
433 (MEK1/2 and ERK1/2) may represent critical nodes of the biological responses of the host
434 during MERS-CoV infection and may be the most logical targets for therapeutic intervention.
435 We also examined inhibitors of Raf, a MAP3K found downstream of the Ras family of

436 membrane GTPases, as Raf was found as an intermediate in upregulated signaling pathways at
437 all time points in our analysis and treatment of cells with GW5074 inhibited MERS-CoV
438 infection (Figure 3A). Pre-treatment with sorafenib strongly inhibited MERS-COV infection
439 (93%) providing further support for a role for the ERK/MAPK signaling pathway during viral
440 infection. The inhibitory activity was reduced when sorafenib was added to cells 2 hr following
441 infection (<30% at the highest concentration tested) suggesting that the role for Raf may be
442 related primarily to processes early in the viral life cycle (viral entry, uptake or uncoating of
443 virions) rather than in viral replication. Dabrafenib, an inhibitor that also targets Raf, had
444 reduced inhibitory activity against MERS-CoV as compared to sorafenib (45%) when added to
445 cells prior to MERS-CoV infection. As with sorafenib, the inhibitory activity of dabrafenib
446 against MERS-CoV was largely negated when added to cells post-infection (Figure 5B)
447 providing further mechanistic evidence for a role for Raf primarily in early viral entry or post-
448 entry events.

449 From the perspective of PI3K/AKT/mTOR signaling, we also investigated licensed
450 inhibitors that targeted AKT or mTOR. Everolimus, an inhibitor of mTOR, largely retained
451 inhibitory activity against MERS-CoV whether added pre- or post-infection (56% and 59%
452 inhibition, respectively at 10 μM) (Figure 5A). These results were very similar to those for
453 rapamycin (sirolimus; Figure 3A and 3B) and provide strong evidence for a critical role for
454 mTOR in MERS-CoV infection. In contrast, miltefosine, an inhibitor of AKT approved for use
455 leishmania, (33), had minimal inhibitory activities against MERS-CoV (28%) at the highest
456 concentration tested when added pre-infection. These activities were completely abrogated when
457 added post-infection (Figure 4B). As the inhibitory activities of everolimus were significantly
458 greater than that of miltefosine at all concentrations ($p<0.05$), this provided further support for a

459 critical role for mTOR within the PI3K/AKT/mTOR signaling pathway in the exacerbation of
460 MERS-COV infection . The results for selumetinib, trametinib and everolimus were also
461 confirmed by traditional plaque reduction assays. HUH7 cells were pre-treated for 1 hr with each
462 of the three inhibitors (10 μM) and then infected at an MOI of 0.05, as per the initial kinome
463 experiments. Following infection, cells were washed and replaced with either media alone
464 (Supplemental Figure 2A) or with media and re-addition of inhibitor at the same concentration as
465 the pre-infection treatments (Supplemental Figure 2B). A single pre-addition of either
466 selumetinib or trametinib resulted in a significant decrease in viral titers and the re-
467 administration of inhibitor following infection (similar to the conditions for the cell-based
468 ELISA experiments) resulted in significant inhibition of viral replication for all three inhibitors.
469
470 **Discussion:**
471 Concerns have been raised regarding the potential global implications of MERS-CoV as
472 an emerging pathogen. As a result of this, there has been great interest in both increasing our
473 understanding of the molecular pathogenesis associated with MERS-CoV infections as well as
474 the identification of potential therapeutic treatment options. Further, there is great interest in
475 characterizing the molecular events that underlie host responses to MERS-CoV and the relation
476 of these to disease pathogenesis and severity.
477 We, and others, have demonstrated the utility of kinome analysis for characterizing the
478 molecular host response to viral infection through the identification of cell signaling networks or
479 individual kinases that are uniquely modulated during these events (22, 34). Kinases are of
480 critical importance to many biological processes and form an important mechanism for the
481 regulation of these processes independent of changes in transcription or translation. As the

dysregulation of cellular kinases has been implicated in numerous human malignancies (35), kinases have become an important target for the design and development of novel therapeutics (36, 37). There are currently 26 kinase inhibitors with United States Food and Drug Administration (FDA) licensure and a continually increasing number at various stages of clinical development. It should also be appreciated that the escalating costs of moving a new drug from bench to bedside (estimated at >$1 billion US) have prompted calls for the investigation and potential repurposing of licensed therapeutics for alternative uses. Thus, kinome analysis provides a unique opportunity to characterize the molecular host response in the investigation of viral infections, including high-consequence pathogens. Here, we employed systems kinome analysis with peptide arrays to characterize the host response to MERS-CoV infection in HUH7 cells, a human hepatoma cell line that is highly permissive to MERS-CoV infection (27).

Our kinome analysis and subsequent pathway and functional network analyses demonstrated that MERS-CoV infection resulted in the selective modulation of ERK/MAPK and PI3K/AKT/mTOR signaling responses throughout the course of infection. Recently, Josset et al. used an inverse genomic signature approach in their transcriptome analysis of MERS-CoV infection *in vitro* for the identification of potential drug targets (20). Our results compliment those recently reported by Josset et al. in regards to the potential of kinase inhibitors as novel treatment strategies for MERS-CoV infection. The transcriptome analysis performed by the authors resulted in the prediction of two kinase inhibitors, LY294002 (PI3K) and SB203580 (p38 MAPK), as potential modulators of MERS-CoV infection. Here, we have employed kinome analysis to provide critical data regarding the functional response of the host to viral infection through the analysis of the activation states of host kinases and cell signaling networks. Further, we have utilized this information for the logical prediction of host kinases that may serve as

505 novel therapeutic targets for MERS-CoV infection. However, our analysis has expanded on these
506 observations by providing functional evidence for the temporal roles of these signaling pathways
507 in the host response during MERS-CoV infection (20).

508 We have demonstrated through systems-level analysis of our kinome data that multiple
509 ERK/MAPK and PI3K/AKT/mTOR family members formed central components of functional
510 networks and signaling pathways throughout the course of our investigation. In addition,
511 ERK/MAPK and PI3K/AKT/mTOR signaling responses were over-represented in our pathway
512 and network analyses, including the functional network derived from the kinases that were
513 conserved across all of the time point examined in our investigation (Supplemental Figure 1),
514 ERK/MAPK and PI3K/AKT/mTOR signaling networks are critical regulatory pathways for
515 many cell regulatory responses including cell proliferation and apoptosis and have been
516 demonstrated to be targeted by a broad range of viral pathogens (38-40). This would suggest that
517 both ERK/MAPK and PI3K/AKT/mTOR signaling responses play important roles in the host
518 response to MERS-CoV infection. Our kinome data, and subsequent pathway and functional
519 network analyses, was corroborated by the phosphorylation patterns of specific members of these
520 pathways by western blot array analysis. Further, the activation of mTOR-regulated intracellular
521 kinases, including S6RP and p70S6K, lends further credence to our pathway and functional
522 network data. In addition to these findings, our analyses also suggested that PKC-mediated
523 signaling also formed important components of the host response to MERS-CoV infection as
524 PKC formed components of both the functional and signaling pathway networks found in our
525 investigation and the inhibition of PKC-mediated signaling responses resulted in decreased
526 MERS-CoV infection whether added pre- or post-infection. As PKC can activate ERK/MAPK
527 signaling (41) these results may provide additional information regarding the mechanism

528 whereby MERS-CoV modulates ERK/MAPK signaling. Prior analysis of MERS-CoV infection
529 have also suggested that IFN responses, and in particular those of IFN-β, play important roles
530 during the course of infection (17). Our analysis demonstrated that IFN-related signaling
531 responses were formed portions of the functional networks found at the 1hr p.i. time point and as
532 well were found in the downregulated signaling pathways at the 24 hr p.i. time point. These
533 observations lend further credence to the growing evidence for a specific attenuation of IFN
534 responses during MERS-CoV infection (17, 18, 42).

535 There has been considerable analysis of the therapeutic potential for host-targeted
536 immunomodulatory agents in viral infections (20, 43, 44). Previous work has demonstrated that
537 viruses modulate host cell signaling networks including PI3K/AKT/mTOR and ERK/MAPK.
538 Human papillomavirus (HPV) is able to maintain an activated AKT resulting in activated
539 mTORC1 and it has been postulated that this may be required for the initiation of viral
540 replication (45). A similar requirement for activated PI3K/AKT/mTOR signaling in viral
541 replication has also been demonstrated for Myxoma virus (46). Qin et al. have also demonstrated
542 that herpes simplex virus type 1 infection stimulated both the PI3K/AKT and ERK/MAPK
543 signaling pathways (47) and the role of ERK/MAPK signaling modulation in viral infection has
544 also been noted for reovirus (48), rabies virus (49) and hepatitis B (50), amongst others. We
545 demonstrated that multiple licensed kinase inhibitors targeting the ERK/MAPK or
546 PI3K/AKT/mTOR signaling pathways inhibited MERS-CoV infection *in vitro* when added prior
547 to or following viral infection. Inhibitors of MEK1/2 (trametinib) and/or ERK1/2 (selumetinib)
548 had the strongest and most conserved inhibitory activities suggesting that MEK1/2 and ERK1/2
549 may have unique capabilities as stand-alone or combinatorial therapies for MERS-CoV
550 infections. Further, both ERK/MAPK intermediates were represented across all time points in

551 signaling pathways or functional networks that were derived from our kinome analysis. These
552 analyses also suggested that mTOR was highly over-represented within our kinome data.
553 Inhibitors of mTOR (rapamycin and everolimus) had reduced inhibitory activities against
554 MERS-CoV as compared to trametinib and selumetinib. However, the conservation of these
555 activities following pre- or post-infection also suggest that mTOR plays a critical role in MERS-
556 COV infections beyond viral entry. Although our kinome data suggested that PI3K could be an
557 attractive therapeutic target for MERS-CoV and treatment of cells with wortmannin, a selective
558 PI3K inhibitor, inhibited MERS-CoV infection, the administration of miltefosine [an AKT
559 inhibitor licensed for use as an anti-leishmanial agent (33)] had minimal inhibitory activity in our
560 analysis. These results suggest that mTOR is likely preferentially modulated during MERS-CoV
561 infection as compared to other PI3K/AKT/mTOR pathway intermediates and, in addition to
562 trametinib and selumetinib, may also represent a logical therapeutic target for MERS-CoV
563 infections. These results were further validated by the significant reduction in viral titers
564 demonstrated when cells were treated for only 1 hr prior to infection (trametinib and selumetinib)
565 or when inhibitors were replenished following infection (trametinib, selumetinib and everolimus)
566 by plaque reduction assay. The specific mechanism(s) of inhibition for these inhibitors remains
567 to be determined. Though it is postulated that this inhibitory effect is mitigated through direct
568 inactivation of the primary targets of these inhibitors it is appreciated that many licensed kinase
569 inhibitors have off-site targets that could contribute to the overall antiviral activities reported
570 here. Specific inhibition of intermediates from the ERK/MAPK and PI3K/AKT/mTOR signaling
571 through approaches such as siRNA knockdown or gene knockout studies will help shed light on
572 this question. Althugh it is tempting to speculate that these compounds may have future
573 therapeutic potential for MERS-CoV infections this will require additional investigations

574 regarding their associated pharmacokinetics and the correlation of these with the levels required
575 for antiviral activity *in vivo*. Future investigations will expand on these findings to determine the
576 precise mechanism of action for these inhibitors in the MERS-CoV viral life cycle (ie. inhibition
577 of viral replication, viral assembly or viral egress).

578 Using kinome analysis, we have demonstrated that MERS-CoV infection resulted in the
579 selective modulation of ERK/MAPK and PI3K/AKT/mTOR signaling responses in the host and
580 confirmed this through biological validation experiments with kinase inhibitors. Further, we have
581 also demonstrated the utility of temporal kinome analysis for characterizing host responses to
582 infection and for the subsequent selection of therapeutics that may provide resolution from
583 infection. Taken together, we provide critical information regarding the molecular host response
584 to MERS-CoV infection and evidence for the potential of kinase inhibitor therapeutics with pre-
585 existing licensure as novel treatment strategies for MERS-CoV infections.

586

587 **Acknowledgments:**

588 This study was supported in part by the NIAID Division of Intramural Research. BJH, JD and
589 JHK performed this work as employees of Tunnell Consulting, Inc, and DT and SM performed
590 this work as employees of MRI Global, subcontractors to Battelle Memorial Institute; and JK,
591 BO and MH performed this work as employees of Battelle Memorial Institute; all under its prime
592 contract with NIAID, under Contract No. HHSN272200700016I.

593

594 **References:**

595 1. **Zaki AM, van Boheemen S, Bestebroer TM, Osterhaus AD, Fouchier RA.** 2012.
596 Isolation of a novel coronavirus from a man with pneumonia in Saudi Arabia. The New
597 England journal of medicine **367:**1814-1820.

2. **Raj VS, Osterhaus AD, Fouchier RA, Haagmans BL.** 2014. MERS: emergence of a novel human coronavirus. Current opinion in virology **5C:**58-62.
3. **Bialek SR, Allen D, Alvarado-Ramy F, Arthur R, Balajee A, Bell D, Best S, Blackmore C, Breakwell L, Cannons A, Brown C, Cetron M, Chea N, Chommanard C, Cohen N, Conover C, Crespo A, Creviston J, Curns AT, Dahl R, Dearth S, DeMaria A, Echols F, Erdman DD, Feikin D, Frias M, Gerber SI, Gulati R, Hale C, Haynes LM, Heberlein-Larson L, Holton K, Ijaz K, Kapoor M, Kohl K, Kuhar DT, Kumar AM, Kundich M, Lippold S, Liu L, Lovchik JC, Madoff L, Martell S, Matthews S, Moore J, Murray LR, Onofrey S, Pallansch MA, Pesik N, Pham H, Pillai S, Pontones P, Pringle K, Pritchard S, Rasmussen S, Richards S, Sandoval M, Schneider E, Schuchat A, Sheedy K, Sherin K, Swerdlow DL, Tappero JW, Vernon MO, Watkins S, Watson J, Division of Viral Diseases NCfI, Respiratory Diseases CDC.** 2014. First Confirmed Cases of Middle East Respiratory Syndrome Coronavirus (MERS-CoV) Infection in the United States, Updated Information on the Epidemiology of MERS-CoV Infection, and Guidance for the Public, Clinicians, and Public Health Authorities - May 2014. MMWR. Morbidity and mortality weekly report **63:**431-436.
4. **Peiris JS, Yuen KY, Osterhaus AD, Stohr K.** 2003. The severe acute respiratory syndrome. The New England journal of medicine **349:**2431-2441.
5. **Pyrc K, Sims AC, Dijkman R, Jebbink M, Long C, Deming D, Donaldson E, Vabret A, Baric R, van der Hoek L, Pickles R.** 2010. Culturing the unculturable: human coronavirus HKU1 infects, replicates, and produces progeny virions in human ciliated airway epithelial cell cultures. Journal of virology **84:**11255-11263.
6. **Lau SK, Li KS, Tsang AK, Lam CS, Ahmed S, Chen H, Chan KH, Woo PC, Yuen KY.** 2013. Genetic characterization of Betacoronavirus lineage C viruses in bats reveals marked sequence divergence in the spike protein of pipistrellus bat coronavirus HKU5 in Japanese pipistrelle: implications for the origin of the novel Middle East respiratory syndrome coronavirus. Journal of virology **87:**8638-8650.
7. **van Boheemen S, de Graaf M, Lauber C, Bestebroer TM, Raj VS, Zaki AM, Osterhaus AD, Haagmans BL, Gorbalenya AE, Snijder EJ, Fouchier RA.** 2012. Genomic characterization of a newly discovered coronavirus associated with acute respiratory distress syndrome in humans. mBio **3**.
8. **Coleman CM, Frieman MB.** 2013. Emergence of the Middle East respiratory syndrome coronavirus. PLoS pathogens **9:**e1003595.
9. **Alagaili AN, Briese T, Mishra N, Kapoor V, Sameroff SC, de Wit E, Munster VJ, Hensley LE, Zalmout IS, Kapoor A, Epstein JH, Karesh WB, Daszak P, Mohammed OB, Lipkin WI.** 2014. Middle East respiratory syndrome coronavirus infection in dromedary camels in saudi arabia. mBio **5:**e00884-00814.
10. **Ferguson NM, Van Kerkhove MD.** 2014. Identification of MERS-CoV in dromedary camels. The Lancet infectious diseases **14:**93-94.
11. **Zumla AI, Memish ZA.** 2014. Middle East respiratory syndrome coronavirus: epidemic potential or a storm in a teacup? Eur Respir J.
12. **Bermingham A, Chand MA, Brown CS, Aarons E, Tong C, Langrish C, Hoschler K, Brown K, Galiano M, Myers R, Pebody RG, Green HK, Boddington NL, Gopal R, Price N, Newsholme W, Drosten C, Fouchier RA, Zambon M.** 2012. Severe respiratory illness caused by a novel coronavirus, in a patient transferred to the United

Kingdom from the Middle East, September 2012. Euro surveillance : bulletin Europeen sur les maladies transmissibles = European communicable disease bulletin **17:**20290.

13. **Geng H, Tan W.** 2013. A novel human coronavirus: Middle East respiratory syndrome human coronavirus. Science China. Life sciences **56:**683-687.
14. **Al-Tawfiq JA, Memish ZA.** 2014. What are our pharmacotherapeutic options for MERS-CoV? Expert review of clinical pharmacology **7:**235-238.
15. **Zielecki F, Weber M, Eickmann M, Spiegelberg L, Zaki AM, Matrosovich M, Becker S, Weber F.** 2013. Human cell tropism and innate immune system interactions of human respiratory coronavirus EMC compared to those of severe acute respiratory syndrome coronavirus. J Virol **87:**5300-5304.
16. **Kindler E, Jonsdottir HR, Muth D, Hamming OJ, Hartmann R, Rodriguez R, Geffers R, Fouchier RA, Drosten C, Muller MA, Dijkman R, Thiel V.** 2013. Efficient replication of the novel human betacoronavirus EMC on primary human epithelium highlights its zoonotic potential. mBio **4:**e00611-00612.
17. **Hart BJ, Dyall J, Postnikova E, Zhou H, Kindrachuk J, Johnson RF, Olinger GG, Jr., Frieman MB, Holbrook MR, Jahrling PB, Hensley L.** 2014. Interferon-beta and mycophenolic acid are potent inhibitors of Middle East respiratory syndrome coronavirus in cell-based assays. J Gen Virol **95:**571-577.
18. **Chan JF, Chan KH, Kao RY, To KK, Zheng BJ, Li CP, Li PT, Dai J, Mok FK, Chen H, Hayden FG, Yuen KY.** 2013. Broad-spectrum antivirals for the emerging Middle East respiratory syndrome coronavirus. J Infect **67:**606-616.
19. **Falzarano D, de Wit E, Martellaro C, Callison J, Munster VJ, Feldmann H.** 2013. Inhibition of novel beta coronavirus replication by a combination of interferon-alpha2b and ribavirin. Scientific reports **3:**1686.
20. **Josset L, Menachery VD, Gralinski LE, Agnihothram S, Sova P, Carter VS, Yount BL, Graham RL, Baric RS, Katze MG.** 2013. Cell host response to infection with novel human coronavirus EMC predicts potential antivirals and important differences with SARS coronavirus. mBio **4:**e00165-00113.
21. **Clarke P, Leser JS, Bowen RA, Tyler KL.** 2014. Virus-induced transcriptional changes in the brain include the differential expression of genes associated with interferon, apoptosis, interleukin 17 receptor A, and glutamate signaling as well as flavivirus-specific upregulation of tRNA synthetases. mBio **5:**e00902-00914.
22. **Kindrachuk J, Arsenault R, Kusalik A, Kindrachuk KN, Trost B, Napper S, Jahrling PB, Blaney JE.** 2012. Systems kinomics demonstrates Congo Basin monkeypox virus infection selectively modulates host cell signaling responses as compared to West African monkeypox virus. Mol Cell Proteomics **11:**M111 015701.
23. **Maattanen P, Trost B, Scruten E, Potter A, Kusalik A, Griebel P, Napper S.** 2013. Divergent immune responses to Mycobacterium avium subsp. paratuberculosis infection correlate with kinome responses at the site of intestinal infection. Infection and immunity **81:**2861-2872.
24. **Mulongo M, Prysliak T, Scruten E, Napper S, Perez-Casal J.** 2014. In vitro infection of bovine monocytes with Mycoplasma bovis delays apoptosis and suppresses production of gamma interferon and tumor necrosis factor alpha but not interleukin-10. Infection and immunity **82:**62-71.
25. **Cohen P.** 2002. Protein kinases--the major drug targets of the twenty-first century? Nat Rev Drug Discov **1:**309-315.

26. **Hopkins AL, Groom CR.** 2002. The druggable genome. Nat Rev Drug Discov **1:**727-730.
27. **de Wilde AH, Raj VS, Oudshoorn D, Bestebroer TM, van Nieuwkoop S, Limpens RW, Posthuma CC, van der Meer Y, Barcena M, Haagmans BL, Snijder EJ, van den Hoogen BG.** 2013. MERS-coronavirus replication induces severe in vitro cytopathology and is strongly inhibited by cyclosporin A or interferon-alpha treatment. J Gen Virol **94:**1749-1760.
28. **de Wit E, Rasmussen AL, Falzarano D, Bushmaker T, Feldmann F, Brining DL, Fischer ER, Martellaro C, Okumura A, Chang J, Scott D, Benecke AG, Katze MG, Feldmann H, Munster VJ.** 2013. Middle East respiratory syndrome coronavirus (MERS-CoV) causes transient lower respiratory tract infection in rhesus macaques. Proceedings of the National Academy of Sciences of the United States of America **110:**16598-16603.
29. **Li Y, Arsenault RJ, Trost B, Slind J, Griebel PJ, Napper S, Kusalik A.** 2012. A systematic approach for analysis of peptide array kinome data. Sci Signal **5:**pl2.
30. **Trost B, Kindrachuk J, Maattanen P, Napper S, Kusalik A.** 2013. PIIKA 2: an expanded, web-based platform for analysis of kinome microarray data. PloS one **8:**e80837.
31. **Lynn DJ, Winsor GL, Chan C, Richard N, Laird MR, Barsky A, Gardy JL, Roche FM, Chan TH, Shah N, Lo R, Naseer M, Que J, Yau M, Acab M, Tulpan D, Whiteside MD, Chikatamarla A, Mah B, Munzner T, Hokamp K, Hancock RE, Brinkman FS.** 2008. InnateDB: facilitating systems-level analyses of the mammalian innate immune response. Mol Syst Biol **4:**218.
32. **Schneider CA, Rasband WS, Eliceiri KW.** 2012. NIH Image to ImageJ: 25 years of image analysis. Nature methods **9:**671-675.
33. **Dorlo TP, Balasegaram M, Beijnen JH, de Vries PJ.** 2012. Miltefosine: a review of its pharmacology and therapeutic efficacy in the treatment of leishmaniasis. J Antimicrob Chemother **67:**2576-2597.
34. **Bowick GC, Fennewald SM, Scott EP, Zhang L, Elsom BL, Aronson JF, Spratt HM, Luxon BA, Gorenstein DG, Herzog NK.** 2007. Identification of differentially activated cell-signaling networks associated with pichinde virus pathogenesis by using systems kinomics. Journal of virology **81:**1923-1933.
35. **Knuutila S, Bjorkqvist AM, Autio K, Tarkkanen M, Wolf M, Monni O, Szymanska J, Larramendy ML, Tapper J, Pere H, El-Rifai W, Hemmer S, Wasenius VM, Vidgren V, Zhu Y.** 1998. DNA copy number amplifications in human neoplasms: review of comparative genomic hybridization studies. The American journal of pathology **152:**1107-1123.
36. **Cohen P.** 2002. Protein kinases--the major drug targets of the twenty-first century? Nature reviews. Drug discovery **1:**309-315.
37. **Hopkins AL, Groom CR.** 2002. The druggable genome. Nature reviews. Drug discovery **1:**727-730.
38. **Ji WT, Liu HJ.** 2008. PI3K-Akt signaling and viral infection. Recent Pat Biotechnol **2:**218-226.
39. **Ehrhardt C, Ludwig S.** 2009. A new player in a deadly game: influenza viruses and the PI3K/Akt signalling pathway. Cell Microbiol **11:**863-871.

40. **Pleschka S.** 2008. RNA viruses and the mitogenic Raf/MEK/ERK signal transduction cascade. Biol Chem **389:**1273-1282.
41. **Ueda Y, Hirai S, Osada S, Suzuki A, Mizuno K, Ohno S.** 1996. Protein kinase C activates the MEK-ERK pathway in a manner independent of Ras and dependent on Raf. The Journal of biological chemistry **271:**23512-23519.
42. **Falzarano D, de Wit E, Rasmussen AL, Feldmann F, Okumura A, Scott DP, Brining D, Bushmaker T, Martellaro C, Baseler L, Benecke AG, Katze MG, Munster VJ, Feldmann H.** 2013. Treatment with interferon-alpha2b and ribavirin improves outcome in MERS-CoV-infected rhesus macaques. Nature medicine.
43. **Ludwig S.** 2011. Disruption of virus-host cell interactions and cell signaling pathways as an anti-viral approach against influenza virus infections. Biol Chem **392:**837-847.
44. **Tisoncik JR, Korth MJ, Simmons CP, Farrar J, Martin TR, Katze MG.** 2012. Into the eye of the cytokine storm. Microbiol Mol Biol Rev **76:**16-32.
45. **Buchkovich NJ, Yu Y, Zampieri CA, Alwine JC.** 2008. The TORrid affairs of viruses: effects of mammalian DNA viruses on the PI3K-Akt-mTOR signalling pathway. Nat Rev Microbiol **6:**266-275.
46. **Wang G, Barrett JW, Stanford M, Werden SJ, Johnston JB, Gao X, Sun M, Cheng JQ, McFadden G.** 2006. Infection of human cancer cells with myxoma virus requires Akt activation via interaction with a viral ankyrin-repeat host range factor. Proceedings of the National Academy of Sciences of the United States of America **103:**4640-4645.
47. **Qin D, Feng N, Fan W, Ma X, Yan Q, Lv Z, Zeng Y, Zhu J, Lu C.** 2011. Activation of PI3K/AKT and ERK MAPK signal pathways is required for the induction of lytic cycle replication of Kaposi's sarcoma-associated herpesvirus by herpes simplex virus type 1. BMC Microbiol **11:**240.
48. **Norman KL, Hirasawa K, Yang AD, Shields MA, Lee PW.** 2004. Reovirus oncolysis: the Ras/RalGEF/p38 pathway dictates host cell permissiveness to reovirus infection. Proceedings of the National Academy of Sciences of the United States of America **101:**11099-11104.
49. **Nakamichi K, Inoue S, Takasaki T, Morimoto K, Kurane I.** 2004. Rabies virus stimulates nitric oxide production and CXC chemokine ligand 10 expression in macrophages through activation of extracellular signal-regulated kinases 1 and 2. J Virol **78:**9376-9388.
50. **Chung TW, Lee YC, Kim CH.** 2004. Hepatitis B viral HBx induces matrix metalloproteinase-9 gene expression through activation of ERK and PI-3K/AKT pathways: involvement of invasive potential. FASEB J **18:**1123-1125.

**Figure Legends:**

**Figure 1: Heatmaps and Hierarchical Clustering of Host Kinome Responses to MERS-CoV Infection.** Peptide phosphorylation was assessed by densitometry, scaled and normalized using GeneSpring 6.0 software. For hierarchical clustering, (1 - Pearson Correlation) was used as the

distance metric and the McQuitty method was used as the linkage method. A) Hierarchical clustering of the MERS-CoV-infected kinome datasets alongside the mock-infected control datasets. B) Cluster analysis of the MERS-CoV-infected kinome datasets following background subtraction of the time-matched mock-infected control datasets. Spots demonstrating a significant differential phosphorylation between the MERS-CoV-infected and mock-infected control were compiled into a dataset for each time point for comparative analysis. The lines at the top of the heatmap indicate the relative similarity between the conditions as listed along the bottom edge of the heatmap. Line length indicates the degree of similarity with shorter lines equating to stronger similarity. The lines on the left side of the heatmap indicate the relative similarity in signal between the 300 individual peptide targets on the arrays. C) Principal component analysis of the mock- and MERS-CoV-infected kinome datasets. D. MERS-CoV titers from infected cells at each time point during the experiment.

**Figure 2: Functional Network Analysis of Temporal Kinome Responses to MERS-CoV Infection in HUH7 Cells.** Following PIIKA analysis, kinome data sets comparing MERS-CoV-infected cells to mock-infected cells were uploaded to IPA for functional network analysis to identify kinases of potential pharmacological interest. The top two functional networks from each time point are presented. A) 1 hr Post-Infection: i. Network 1: Cell morphology, cellular function and maintenance, carbohydrate metabolism; ii. Network 2: Embryonic development, organ development, organismal development. B) 6 hr Post-Infection: i. Network 1: Gene expression, RNA damage and repair, RNA post-transcriptional modification; ii. Network 2: Cell morphology, cellular function and maintenance, cell cycle. C) 24 hr Post-Infection: i. Network 1:

797 Cancer, hematological disease, cell death and survival; ii. Network 2: Post-translational
798 modification, cell morphology, cellular assembly and organization.
799
800 **Figure 3: Western Blot Array Analysis of Select Phosphorylation Events in MERS-CoV-**
801 **Infected and Mock-Infected Cells.** Pixel intensities for selected spots on the array are presented
802 on the y-axis (arbitrary units). Results are presented as mean ± SD. A) 1hr post-infection. B) 6hr
803 post-infection. C) 24hr post-infection. The results represent one experiment (mean ± SD, n=3)
804 and the experiment was repeated twice.
805
806 **Figure 4: Inhibition of MERS-CoV Infection by Kinase Inhibitors.** Kinase inhibitors were
807 either added pre- (-1hr) or post- (+2hr) infection at the concentrations listed. Results are
808 presented as mean ± SD. A) Pre-infection addition of kinase inhibitors targeting signaling
809 pathways/kinases identified from bioinformatics analysis of temporal kinome data. B) Post-
810 infection addition of kinase inhibitors selected from (A). Cytotoxicities for all compounds at the
811 highest concentration tested (10 μM) were <10%, with the exception of PKC-412 and Ro 31-
812 8220 (20% and 23%, respectively). C) Kinase inhibitor targets from this analysis. The results
813 represent three experimental repeats (mean ± SD, n=3) with two technological repeats performed
814 in each experiment.
815
816 **Figure 5: Inhibitory Activity of FDA-Licensed Kinase Inhibitors Targeting ERK/MAPK or**
817 **PI3K/AKT Signaling Added Pre- or Post- MERS-CoV Infection.** Kinase inhibitors were
818 added pre- (-1 hr) or post (+2 hr) MERS-CoV infection at the concentrations listed. Results are
819 presented as mean ± SD. A) Pre-infection addition of kinase inhibitors targeting signaling

820 pathways/kinases identified from bioinformatics analysis of temporal kinome data. B) Post-
821 infection addition of kinase inhibitors. Cytotoxicities for all compounds tested were <10%. C)
822 Kinase inhibitor targets from this analysis. The results represent three experimental repeats
823 (mean ± SD, n=3) with two technological repeats performed in each experiment.
824 *For the pre-treatment experiments, trametinib was significantly more inhibitory than
825 selumetinib at 0.1 μM ($p<0.05$). For the post-addition experiments, trametinib was significantly
826 more inhibitory than selumetinib at 1 μM ($p<0.005$).

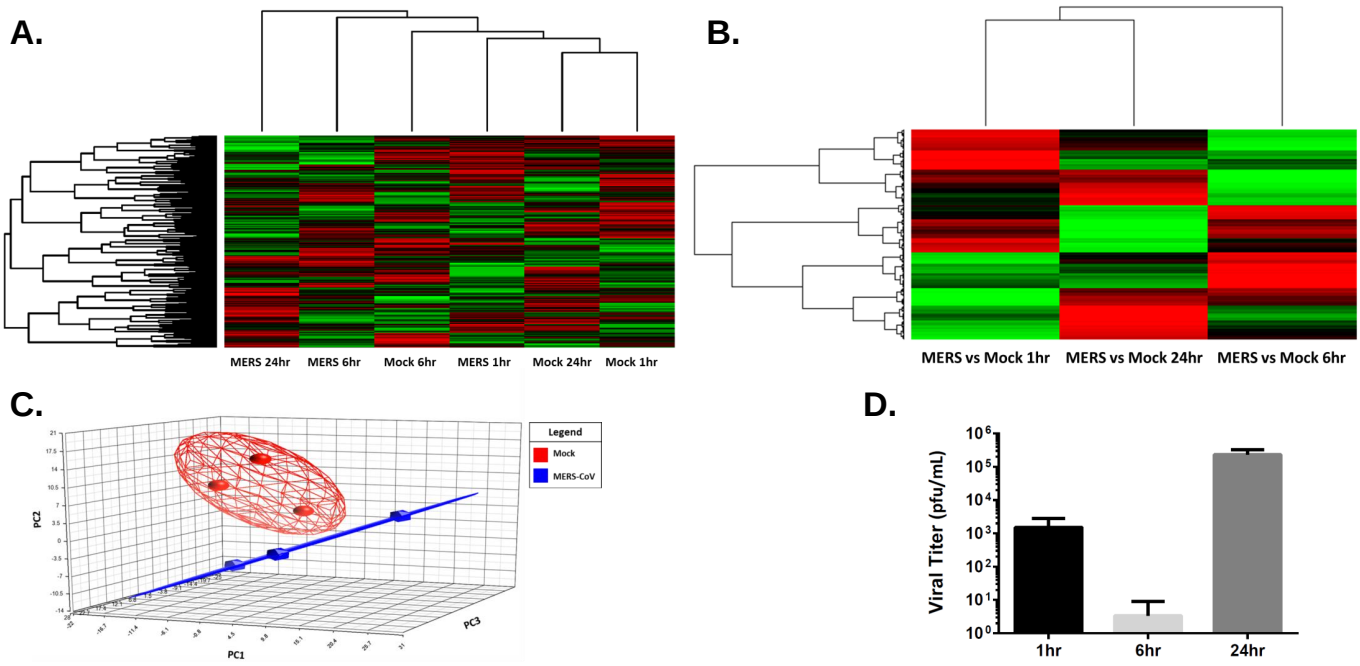


**Figure 1: Heatmaps and Hierarchical Clustering of Host Kinome Responses to MERS-CoV Infection.** Peptide phosphorylation was assessed by densitometry, scaled and normalized using GeneSpring 6.0 software. For hierarchical clustering, (1 - Pearson Correlation) was used as the distance metric and the McQuitty method was used as the linkage method. A) Hierarchical clustering of the MERS-CoV-infected kinome datasets alongside the mock-infected control datasets. B) Cluster analysis of the MERS-CoV-infected kinome datasets following background subtraction of the time-matched mock-infected control datasets. Spots demonstrating a significant differential phosphorylation were compiled into a dataset for each time point for comparative analysis. The lines at the top of the heatmap indicate the relative similarity between the conditions as listed along the bottom edge of the heatmap. Line length indicates the degree of similarity with shorter lines equating to stronger similarity. The lines on the left side of the heatmap indicate the relative similarity in signal between the 300 individual peptide targets on the arrays. C) Principal component analysis of the mock- and MERS-CoV-infected kinome datasets. D. MERS-CoV titers from infected cells at each time point during the experiment.

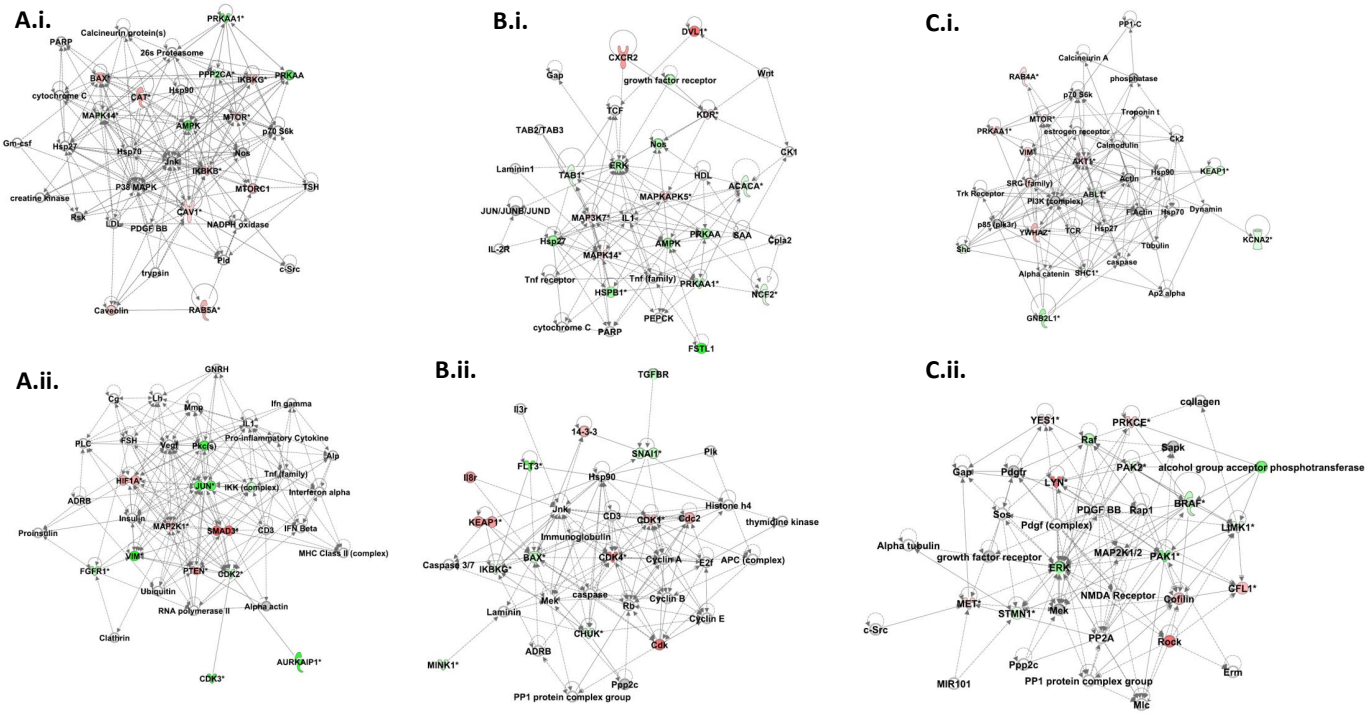


**Figure 2: Functional Network Analysis of Temporal Kinome Responses to MERS-CoV Infection in HUH7 Cells.** Following PIIKA analysis, kinome data sets comparing MERS-CoV-infected cells to mock-infected cells were uploaded to IPA for functional network analysis to identify kinases of potential pharmacological interest. The top two functional networks from each time point are presented. A) 1 hr Post-Infection: i. Network 1: Cell morphology, cellular function and maintenance, carbohydrate metabolism; ii. Network 2: Embryonic development, organ development, organismal development. B) 6 hr Post-Infection: i. Network 1: Gene expression, RNA damage and repair, RNA post-transcriptional modification; ii. Network 2: Cell morphology, cellular function and maintenance, cell cycle. C) 24 hr Post-Infection: i. Network 1: Cancer, hematological disease, cell death and survival; ii. Network 2: Post-translational modification, cell morphology, cellular assembly and organization.

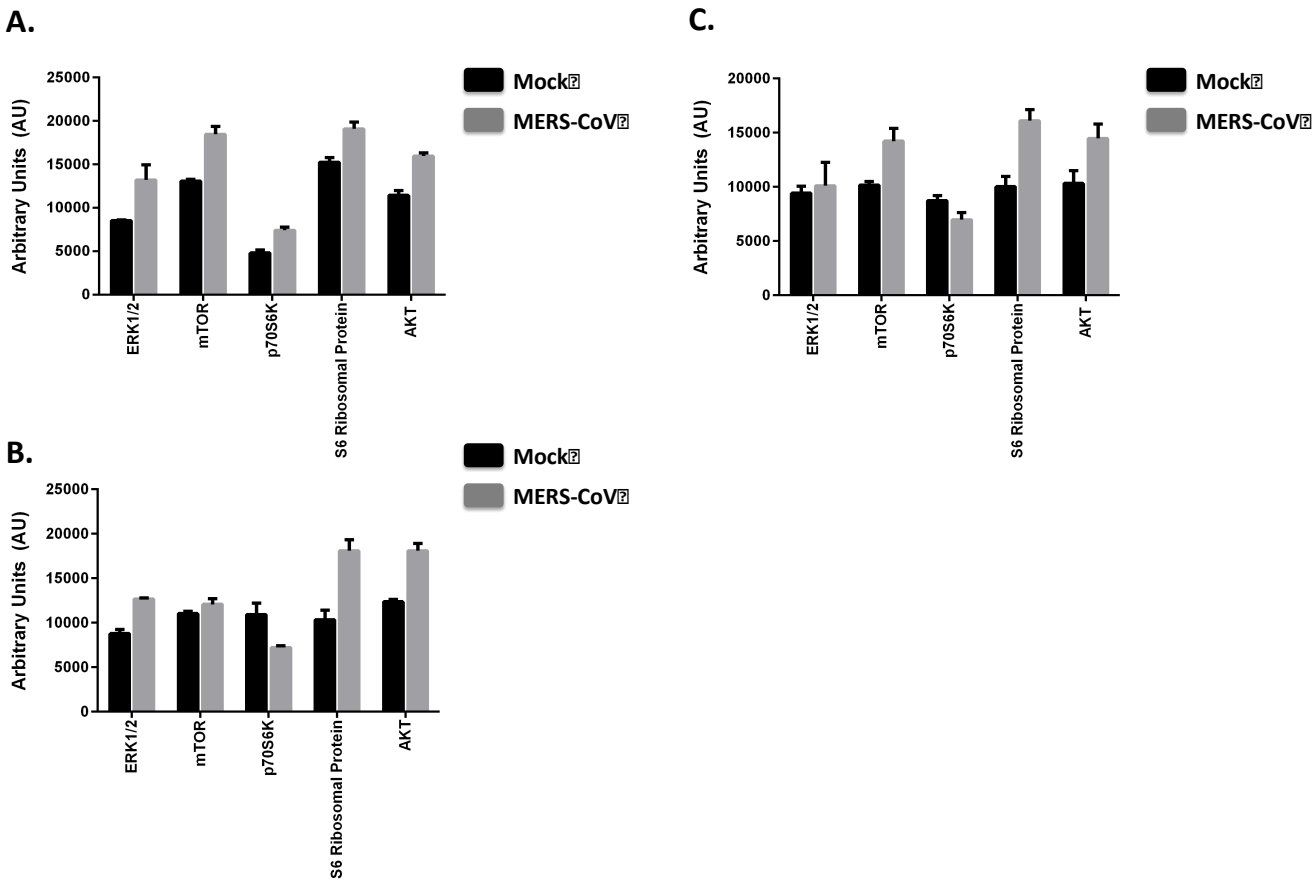


**Figure 3: Western Blot Array Analysis of Select Phosphorylation Events in MERS-CoV-Infected and Mock-Infected Cells.** Pixel intensities for selected spots on the array are presented on the y-axis (arbitrary units). Results are presented as mean ± SD. A) 1hr post-infection. B) 6hr post-infection. C) 24hr post-infection. The results represent one experiment (mean ± SD, n=3) and the experiment was repeated twice.

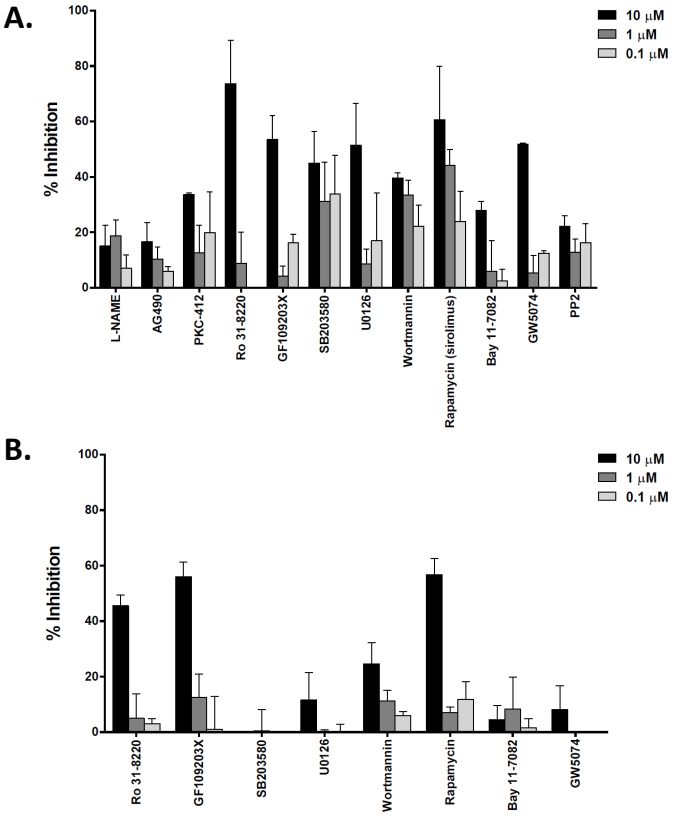


C.

| Inhibitor | Cellular Target |
|---|---|
| L-NAME | nitric oxide synthase |
| AG490 | EGFR; ERBB2 |
| PKC-412 | PKC |
| Ro 31-8220 | PKC |
| GF109203X | PKC |
| SB203580 | p38 MAPK |
| U0126 | MEK1/2 |
| Wortmannin | PI3K |
| Rapamycin | mTOR |
| Bay 11-7082 | IKBα |
| GW5074 | c-Raf1 |
| PP2 | Src |

**Figure 4: Inhibition of MERS-CoV Infection by Kinase Inhibitors.** Kinase inhibitors were either added pre- (-1hr) or post- (+2hr) infection at the concentrations listed. Results are presented as mean ± SD. A) Pre-infection addition of kinase inhibitors targeting signaling pathways/kinases identified from bioinformatics analysis of temporal kinome data. B) Post-infection addition of kinase inhibitors selected from (A). Cytotoxicities for all compounds tested were <10%. C) Kinase inhibitor targets from this analysis.

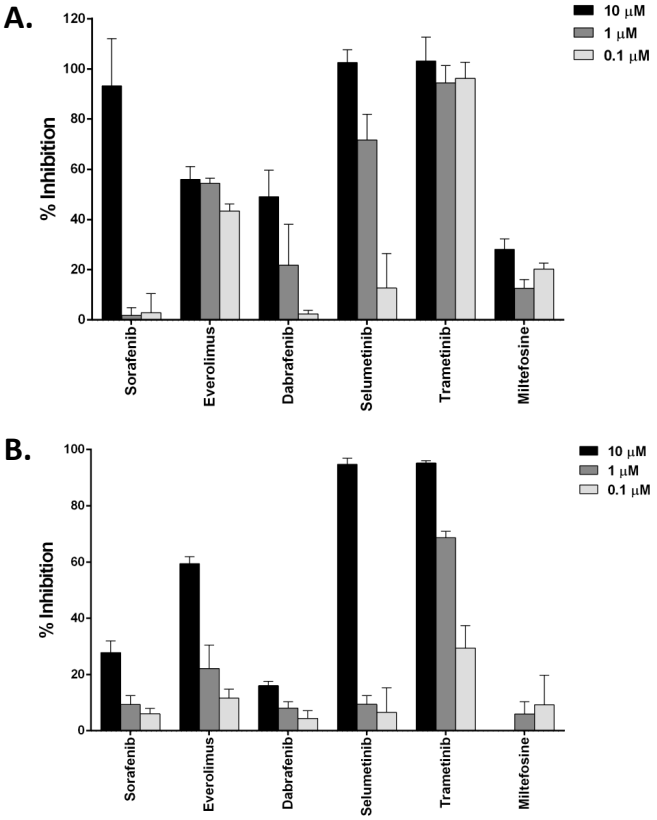


C.

| Inhibitor | Cellular Target |
|---|---|
| Sorafenib | c-Raf; VEGFR; PDGFR |
| Everolimus | mTOR |
| Dabrafenib | B-Raf; C-Raf |
| Selumetinib | MEK1; ERK1/2 |
| Trametinib | MEK1/2 |
| Miltefosine | AKT |

**Figure 5: Inhibitory Activity of FDA-Licensed Kinase Inhibitors Targeting ERK/MAPK or PI3K/AKT Signaling Added Pre- or Post- MERS-CoV Infection.** Kinase inhibitors were added pre- (-1 hr) or post (+2 hr) MERS-CoV infection at the concentrations listed. Results are presented as mean ± SD. A) Pre-infection addition of kinase inhibitors targeting signaling pathways/kinases identified from bioinformatics analysis of temporal kinome data. B) Post-infection addition of kinase inhibitors. Cytotoxicities for all compounds tested were <10%. C) Kinase inhibitor targets from this analysis.